Extended Abstracts of the 2012 International Conference on Solid State Devices and Materials, Kyoto, 2012, pp610-611

Effect of the active layer thickness and temperature on the switching kinetics of GeS_2-based Conductive Bridge Memories

G. Palma[1], E. Vianello[1], G. Molas[1], C. Cagli[1], F. Longnos[2], J. Guy[1], M. Reyboz[1], C. Carabasse[1], M. Bernard[1], F. Dahmani[2], D. Bretegnier[2], J. Liebault[2], B. De Salvo[1]

[1] CEA, LETI, MINATEC Campus, 17 rue des Martyrs, 38054 Grenoble Cedex 9, France
Phone: +330438784056 E-mail: giorgio.palma@cea.fr
[2] Altis Semiconductor, 224 Bd John Kennedy F-91105 Corbeil Essones Cedex

1. Introduction

Conductive Bridge Random Access Memories (CBRAM) are receiving widespread interest as possible FLASH technology replacement for several applications [1-3]. In particular its relatively simple structure and very low power consumption together with high programming speed make this technology suitable for embedded applications [4].

The device working principle relies on the reversible formation of a conductive filament (CF) through a solid electrolyte. The understanding of the filament formation/disruption mechanism is a key step for the development and commercialization of this technology. In our previous work, we investigated the switching kinetics of GeS_2/Ag based CBRAM devices [5]. In this paper, we push further the analysis by addressing the key impact of the temperature and active layer thickness on the SET and RESET characteristics. A numerical model of filament growth/dissolution thermally and field activated is here proposed, able to account for experimental data, clarifying the involved physical processes in the CBRAM operations.

2. Sample description

Fig. 1 shows a schematic representation of the CBRAM device used in this work. A Tungsten (W) plug, with a diameter of 200nm, is used as inert electrode. The solid electrolyte consists of a GeS_2 layer, while a 75nm thick Ag layer is deposited as top electrode. For the purpose of this work, five samples with different GeS_2 thicknesses L (namely S1: 20nm, S2: 30nm, S3: 50nm, S4: 100nm and S5: 150nm) were integrated (see Table 1).

3. Results and discussion

Model description: For the sake of simplicity, we consider the CF as cylindrical, with radius $r(t)$ and height $h(t)$ (Fig. 1). Taking into account the models of [5-6] we described the CF evolution with three stages: 1) the vertical growth; 2) the lateral growth; 3) the lateral dissolution (see Fig. 2). The CF vertical and lateral time evolution are assumed to be proportional to the ion current density and are modeled according to a thermally and field activated hopping model [Eqs. (1) and (2)]. The cell resistance is determined by $r(t)$ and $h(t)$ according to Eq. (3) [7].

Temperature effects: Fig.4 shows the SET resistance (R_{set}) obtained when programming the sample S2 (L=30nm) with different compliance currents. The experiment has been performed at different temperatures, namely 27°C, 85°C and 130°C. At room temperature the dependence of R_{set} on the compliance current follows a power law: $R_{set}=A/(I_{comp})^n$, with n=1. This relationship has been demonstrated [8-9] to be independent of the material composition and the applied (SET) voltage. However, Fig.4 shows that changing the temperatures, the exponent n is no longer equal to 1. For a fixed value of the compliance current, lower resistance values are obtained when increasing the temperature (n decreases with increasing temperature). It is worth noting that the RESET resistance (R_{reset}) is always around 1 GΩ for all temperatures and current compliance values. Fig.5 reports the SET and RESET voltages (V_{set}, V_{reset}) as a function of the temperature (the compliance current was set to 30μA). As temperature increases, the V_{set} decreases while V_{reset} remains almost constant. Note, however, that the impact of the temperature on the V_{reset} is probably hidden by the lower R_{set} (higher I_{reset}) values obtained at high temperatures (see Fig.6). The experimental results are well reproduced by the simulations, thus confirming the hypothesis that the CF time evolution can be assumed proportional to a thermally activated ion hopping current [see Eq.(1) and (2)].

Active layer thickness effects: Increasing the active layer thickness (L) up to 50nm, V_{set} increases. For L higher than 50nm V_{set} seems to saturate (see Fig.7), while $V_{forming}$ (defined for a virgin cell) monotonically increases. These results may be interpreted assuming that for L<50nm, the CF in the OFF state is almost completely dissolved leading to a dependence between V_{set} and the thickness, while for higher L values a portion of the filament might subsist on the W electrode ($h(t=0) \neq 0$) acting as a cathode [10]: thus reducing the distance the ions have to cover in the following SET cycle. In particular, the V_{set} saturation seems to indicate that during the RESET process, up to ~50nm of filament is dissolved, regardless of the GeS_2 thickness (see Fig.8). On the contrary V_{reset} is less sensitive to L (Fig.7), what is in agreement with the constant measured R_{set} value (Fig.9). This can be explained by a lower impact of the electric field on the lateral dissolution during the RESET operation. Fig.10 shows the SET time versus the applied voltage as obtained during programming in the pulsed mode: the sample S2 (L=30nm) shows a lower switching time compared to the S3 (L=50nm) one. The model reproduces the experimental data confirming the hypothesis that for L<50nm, the CF in the OFF state is almost completely dissolved.

4. Conclusions

In summary, we presented a thermally and field activated ion migration model for filament growth/dissolution able to well reproduce switching kinetics of GeS_2-based CBRAM. We demonstrated that as the temperature increases, the SET voltage and resistance decrease. The model also suggests that during the same RESET conditions, for GeS_2 thicknesses lower than 50nm, the CF in the OFF state is almost completely dissolved, while for thicker layers a portion of the filament might subsist.

Table 1: Studied device samples

	S1	S2	S3	S4	S5
L [nm]	20	30	50	100	150

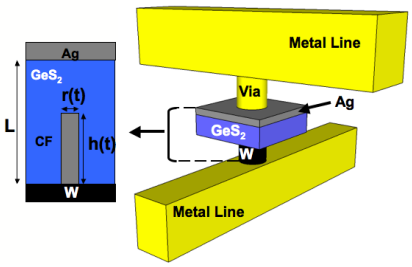

Fig. 1: Schematic view of the CBRAM device. The CF is cylindrical with height *h(t)* and radius *r(t)*.

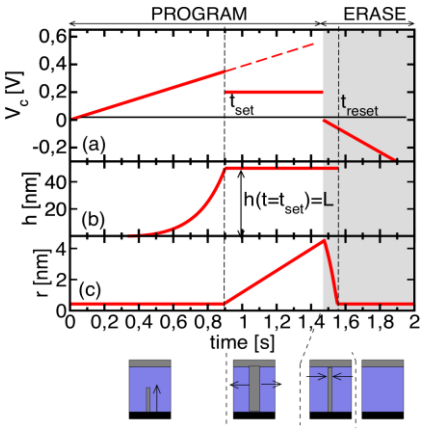

Fig. 2: Simulated sequence of the set and reset transient: (a) up-down voltage sweep applied; (b) vertical and (c) lateral evolution of the CF.

Parameter	Value
v_h	$0.07\ m/s$
v_r	$0.05\ m/s$
ρ_{on} (T = 300 K)	$2.3 \times 10^{-6}\ \Omega\ m$
ρ_{on} (T = 400 K)	$93 \times 10^{-6}\ \Omega\ m$
E_A	$0.4\ eV$
ρ_{off}	$8 \times 10^{3}\ \Omega\ m$
α	0.4
β	0.35
Δ	$0.15\ V$
A	$0.2\ V$

Table 2: Parameters used in the simulations.

$$\frac{dh}{dt} = \frac{J_h(t)}{qN_i} = v_h \exp\left(\frac{-E_A}{k_B T}\right) \sinh\left(\alpha q \frac{V_c(t) - \Delta}{k_B T}\right) \quad (1)$$

$$\frac{dr}{dt} = \frac{J_r(t)}{qN_i} = v_r \exp\left(\frac{-E_A}{k_B T}\right) \sinh\left(\beta q \frac{V_c(t) - \Delta}{k_B T}\right) \quad (2)$$

$$R_c = \frac{\rho_{on} h(t) + \rho_{off}(L - h(t))}{\pi r^2(t)} \quad (3)$$

Fig. 3: Equations used in the model to describe the CF growth (Eq.(1))/dissolution (Eq.(2)) and CF resistance R_c (Eq.(3)).

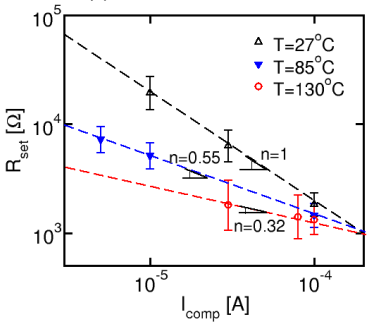

Fig. 4: R_{set} dependence on I_{comp} for different temperatures. The experimental data (symbols) are fitted with $R_{set}=A/I_{comp}^{n}$.

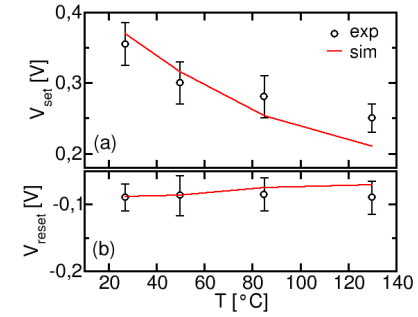

Fig. 5: Experimental (symbols) and simulated (lines) V_{set} (a) and V_{reset} (b) versus temperature.

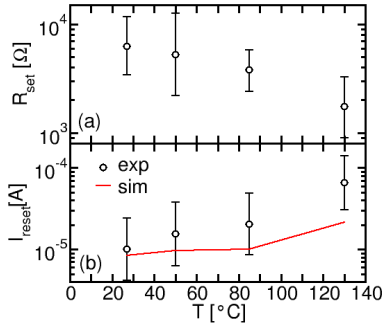

Fig. 6: Experimental (symbols) and simulated (line) R_{set} (a) and I_{reset} (b) versus temperature.

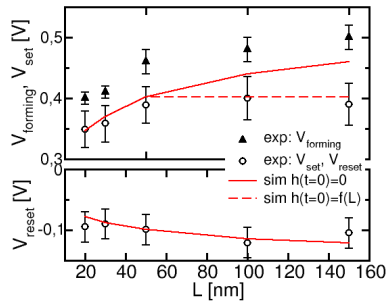

Fig. 7: Experimental (symbols) and simulated (lines) $V_{forming}$, V_{set} (a) and V_{reset} (b) versus L.

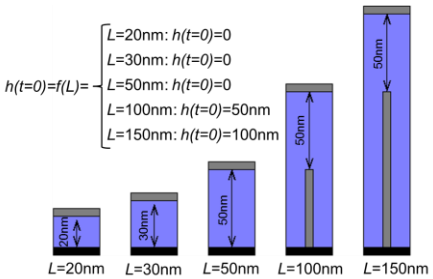

Fig. 8: CF height ($h(t=0)$) at the end of the same RESET process for different L values.

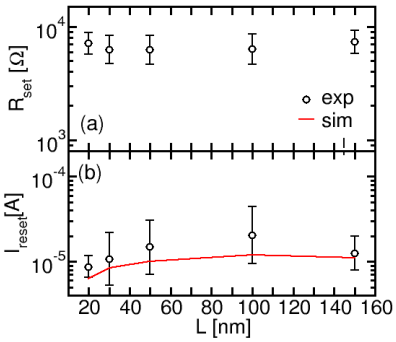

Fig. 9: Experimental (symbols) and simulated (line) R_{set}(a) and I_{reset}(b) versus thickness.

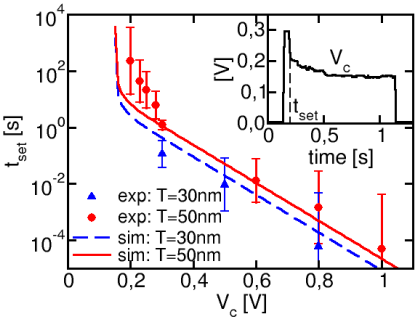

Fig. 10: Experimental (symbols) and simulated (lines) switching time as a function of V_C. Inset: oscilloscope trace of V_C during a pulse-mode set operation.

References

[1] M. Kund et al., IEDM 205, p. 754

[2] T. Tsuruoka et al., Nanotechnology 22, p.254013, 2011.

[3] M. Tada et al., IEDM Tech. Dig. 2009, p.943.

[4] N. Derhacobian et al., Proc. of IEEE, 98, p. 283 (2010)

[5] G. Palma et al., proc. of IMW 2012

[6] S. Yu et al., IEEE Trans. Elec. Dev., 58 (5) pp. 1352-1360

[7] D. B. Strukov et al., Nature, 453, 7191, pp. 80-83 (2008)

[8] I. Valov et al., Nanotechnology 22, pp. 1-22 (2011)

[9] D. Ielmini, IEEE Trans. Elec. Dev., 58 (12) pp. 4309-4317

[10] R. Waser et al., Adv. Mater. 21, pp. 2632-2663 (2009)